

Optical properties and surface morphology of pulsed-laser-deposited polycrystalline PNZT thin films

Jyrki Lappalainen^{a,*}, Vilho Lantto^a, Johannes Frantti^a, Sergey A. Ivanov^b

^a*Microelectronics and Materials Physics Laboratories, PO Box 4500, FIN-90014 University of Oulu, Finland*

^b*Karpov' Institute of Physical Chemistry, X-ray laboratory, 103064, ul. Vorontsovo pole 10, Moscow, Russia*

Received 4 September 2000; received in revised form 23 October 2000; accepted 10 November 2000

Abstract

Pulsed XeCl-excimer laser and Nd-modified lead–zirconate–titanate (PNZT) targets were used for the laser-ablation deposition of PNZT thin films on MgO(100) substrates. Films were post-annealed at 700, 800 and 900°C and optical transmission and reflection spectra were measured. AFM and XRD techniques were used for structural and surface quality characterization. In the films annealed at 700°C, the crystal structure was found to be polycrystalline and the surface quality and optical properties were found to depend also on the laser-beam fluence. However, in the films annealed at 800 and 900°C, a growth of large grains, where the $\langle 001 \rangle$ crystal direction was perpendicular to the film surface, was found. The surface morphology and optical properties of the films were clearly improved. The band-gap energy $E_g \approx 3.5$ eV, refractive index $n \approx 2.1$ and extinction coefficient $k \approx 0.014$ at the wavelength of 600 nm were calculated. © 2001 Elsevier Science Ltd. All rights reserved.

Keywords: Films; Optical properties; Pulsed laser deposition; PZT; Surfaces

1. Introduction

High optical transmittance, low reflectance, and strong electro-optic Kerr effect of ferroelectric lead–zirconate–titanate (PZT) films can be utilized in various optical applications like acoustooptic Bragg deflectors based on SAW technology, light-beam switching shutters, modulators and waveguides. In the Kerr effect, a change of the refractive index, Δn , of the PZT film is proportional to the square of the applied electric field, E^2 , thus making the control of the polarized light propagation in PZT films possible.¹ Especially, it has been reported that La-doped PZT ceramics have excellent optical properties also in the form of thin films.² The transmittance $T(\lambda)$ and reflectance $R(\lambda)$ values of $\text{PbZr}_x\text{Ti}_{1-x}\text{O}_3$ thin films at wavelengths well above the absorption edge varies between 60 and 90% and between 10 and 30%, respectively.^{3,4} The film thickness, crystal structure, orientation of the crystals, grain size distribution, packing density and morphology of the film surface affect strongly on the optical properties of Nd-modified lead–zirconate–titanate (PNZT) thin

films.^{5,6} Some of these parameters depend on film-deposition and heat-treatment processes, to a large extent.

In this paper, some results are presented of optical properties of PNZT thin films grown by the pulsed-laser-deposition (PLD) process at room temperature, and post-annealed afterwards at different temperatures. When the initial composition of the ceramic PNZT target was near to the morphotropic phase boundary (MPB), the laser-beam fluence used for the deposition process was found to affect on the chemical composition of the as-grown amorphous PNZT films.⁷ Furthermore, after annealing procedure the crystal structure of the films depended on the initial zirconium content of amorphous films. Another property of the PLD process, especially when optical applications are considered, is the generation of large particulates in the film, thus impairing the surface morphology of the film. However, as described later in this paper, the annealing process determines mainly the quality of the film surface.^{8,9}

2. Experimental

A pulsed XeCl-excimer laser with a wavelength of 308 nm was used to deposit amorphous PNZT thin films

* Corresponding author. Tel.: +358-8-5532720; fax: +358-8-553 2728.

E-mail address: jyli@ee.oulu.fi (J. Lappalainen).

with thicknesses between 25 and 600 nm on MgO(100) substrates at room temperature.¹⁰ The repetition rate of laser pulses was 25 Hz and the duration of the single pulse was 30 ns. The laser-beam fluence was varied between 0.4 and 2.0 J/cm² and a Pb_{0.97}Nd_{0.02}(Zr_{0.55}Ti_{0.45})O₃ target with a density of 7.4×10³ kg/m³ was used. The target was pressed from a PNZT powder with a mean particle size of 0.5 µm under a pressure of 500 kPa at room temperature. The sintering process was carried out under an inverted zirconia crucible together with some extra PNZT powder, in order to prevent an excess loss of lead, by heating 20 min at a maximum temperature of 1100°C.

After deposition, the PNZT thin films were post-annealed at different temperatures of 700, 800 and 900°C for 20 min under the inverted zirconia crucible together with some PNZT powder. After annealing, the crystal structure and grain size of the PNZT films were determined by X-ray diffraction (XRD) measurements. Atomic force microscopy (AFM), Digital Instruments Nanoscope II, was used to study the surface morphology of both amorphous and annealed thin films. The field emission scanning electron microscopy (FESEM), Jeol JSM-6300F, was also used to study the grain size and the structure of cross sections of the PNZT films.

Optical transmission and reflection spectra in the wavelength range from 250 to 750 nm were measured using a construction composed of a light source with focusing optics (Oriel 66001 Xenon UV-arc-lamp), a monochromator (Jarrel-Ash 82410), a conventional sample holder construction with achromatic focusing optics, and a UV-enhanced silicon PIN-photodiode connected to measurement electronics.¹¹ The measurement system was calibrated with a Hg spectral calibration lamp (Oriel 6050), and a wavelength accuracy of ±4 nm was obtained. Optical constants were calculated using the SCI Film Spectrum version 4.8 software.

AFM pictures were analyzed with the Image SXM version 1.61 software. Amplitude distribution functions (ADF) were formed for picture profiles to describe the statistical distribution of the film surface height data. Based on these data, bearing area curves (BAC) and core-roughness values R_k were calculated in order to evaluate the morphology of the PNZT thin films. Basically, BAC shows the cumulative fraction of the studied film area, which is covered by a certain height of the surface. The core-roughness R_k is a measure describing the height difference range where the maximum gradient in a 40% ordinate range of the BAC curve is found.

3. Results and discussion

The crystal structure and the grain size of the films were studied by XRD measurements. Three XRD patterns from PNZT films with the thickness of around 300

nm and annealed at 700, 800 and 900°C, respectively, are shown in Fig. 1. In the case of the film annealed at 700°C, the XRD pattern is very similar to that measured from the target and do not reveal any specific grain orientation. The intensity in the pattern was very weak and a peak at 2θ angle of 30° shows a possible pyrochlore phase in the structure. Although the overall intensity of the XRD pattern from the film annealed at 800°C is still low, the intensities of the (001) and (002) reflections are clearly pronounced. The increase is an indication of the orientation of grains with increasing annealing temperature so that the <001> direction agrees with the normal direction of the film surface. In the PNZT film annealed at 900°C in Fig. 1, this orientation is already very clear and the majority of grains in the film are oriented with the <001> crystal direction perpendicular to the film surface. The mean grain size of the PNZT films annealed at 700, 800 and 900°C were 210, 250 and 330 Å, respectively.

Two pairs of AFM and FESEM micrographs of the annealed PNZT thin films are shown in Fig. 2. Surface morphology and cross-section images of the PNZT thin film annealed at 700°C are shown in Fig. 2(a) and (b), respectively. Similarly, in Fig. 2(c) and (d) are shown corresponding images of the film annealed at 800°C. In

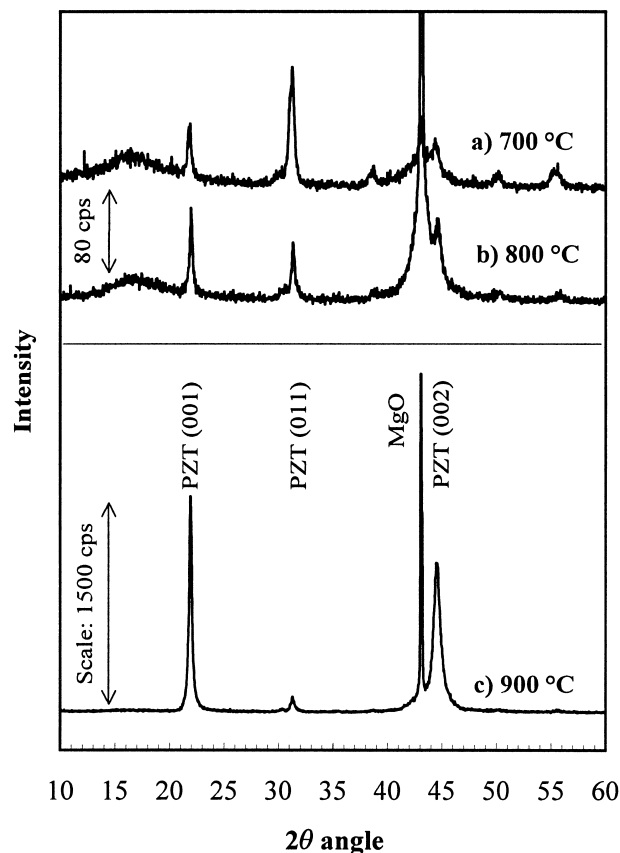


Fig. 1. XRD patterns of three PNZT thin films deposited with a laser-beam fluence of 2.0 J/cm² and annealed at (a) 700, (b) 800 and (c) 900°C. The thickness of the films was about 300 nm.

Fig. 2(a), the presence of large particulates in the film surface is shown. Although the vertical scales in Fig. 2(a) and (c) are different, the strengthening grain growth in the PNZT film annealed at 800°C in comparison to that of the film annealed at 700°C, is shown in Fig. 2(c). This observation is further supported by the cross-section FESEM micrographs in Fig. 2(b) and (d). The film annealed at 700°C had a polycrystalline structure with random grain orientation and quite small grain size. However, two separate layers are already seen in the structure of the PNZT film annealed at 800°C in Fig. 2(d). In the upper surface part of the film, a layer with a columnar grain structure and a thickness of

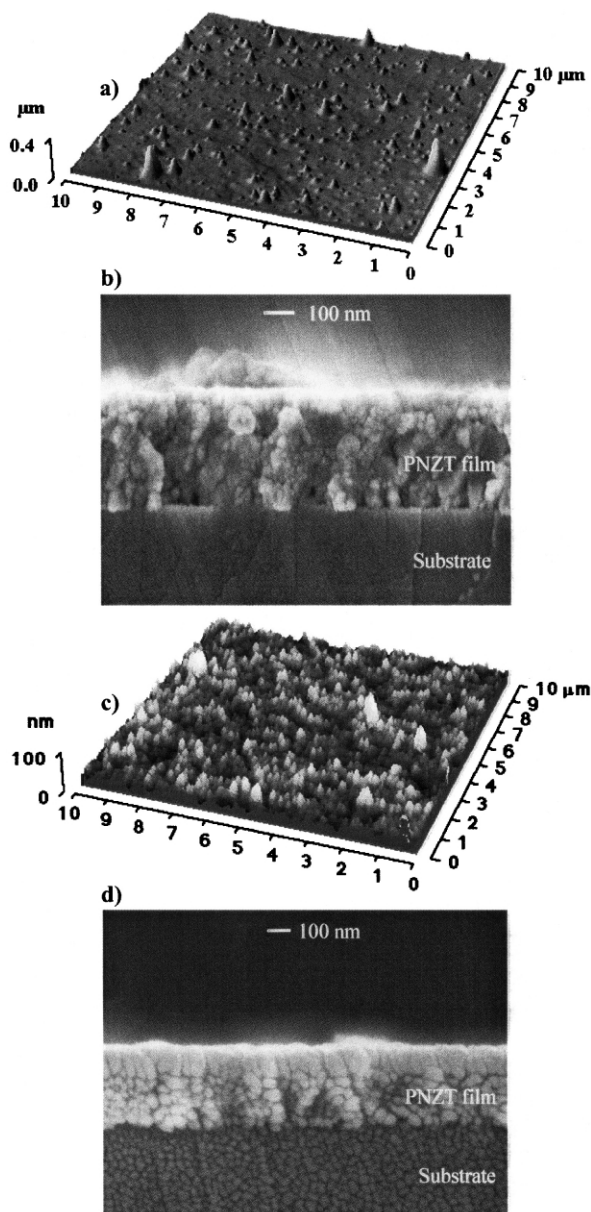


Fig. 2. AFM and FESEM micrographs of PNZT thin film surfaces and cross-sections after annealing at (a), (b) 700°C and (c), (d) 800°C, respectively. In the micrograph (d), the columnar grain growth in the film surface is clearly seen.

around 130 nm is seen to exist. Under this layer, there is a polycrystalline PNZT layer with thickness of 180 nm and a smaller grain-size distribution without any particular orientation in the grain growth.

ADF and the corresponding bearing area curves were calculated from the AFM micrographs. Five BAC of PNZT films annealed at different temperatures are shown in Fig. 3. The abscissa axis shows the variation of the surface height of the film from the maximum value of the ADF. It was found that BAC curves became steeper with increasing annealing temperature from 700 to 800°C, and the R_k values decreased from 91 and 102 nm to 12 and 16 nm, respectively. This result is an indication of the increasing surface flatness of PNZT films with increasing annealing temperature. In the case of amorphous films having typically a quite flat background surface without particulates, R_k had an average value of 28 nm. After annealing at 700°C, our average value of R_k was 98 nm. After annealing at 800°C, however, the average value of R_k was only 15 nm.

Optical transmission $T(\lambda)$ and reflection $R(\lambda)$ spectra measured in UV and visible wavelength ranges from three PNZT films are shown in Fig. 4 together with the transmission spectrum from the MgO(100) substrate with a thickness of 500 μm. Both the transmission and reflection responses were weakest for the films annealed at 700°C and, especially, the amplitude of the interference envelope decreased at shorter wavelengths. The reflectance of the films increased clearly together with increasing annealing temperature, and the films

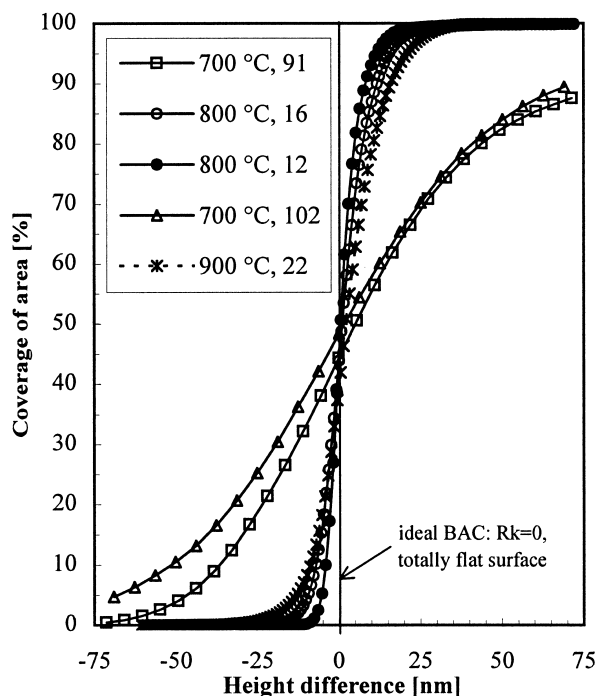


Fig. 3. Bearing area curves with the corresponding values of the core-roughness R_k (in nanometers) of five PNZT thin films annealed at 700, 800 and 900°C, respectively.

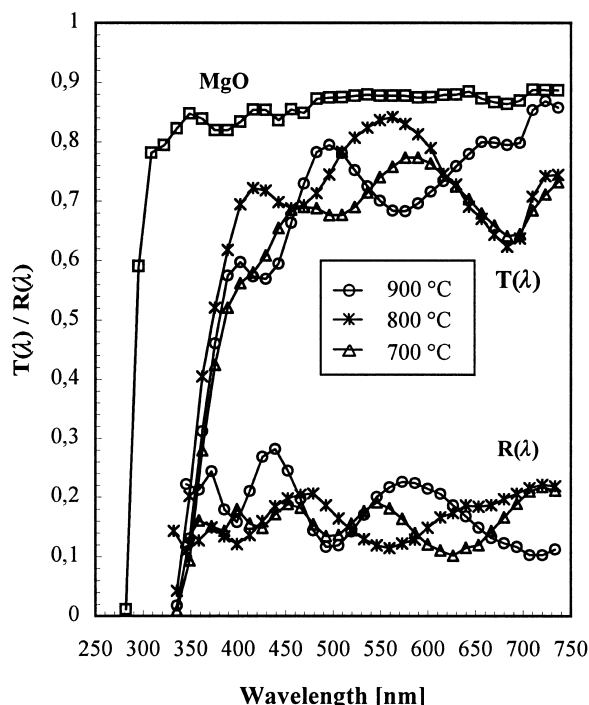


Fig. 4. Optical transmittance $T(\lambda)$ and reflectance $R(\lambda)$ spectra of three PNZT thin films with thicknesses of about 300 nm, and annealed at 700, 800 and 900°C, respectively. Substrate transmission spectrum with an abrupt absorption edge at the wavelength of 290 nm is also shown.

annealed at 900°C had a reflectance value of 0.2 at the wavelengths below 450 nm. Typically, the films which were thinner than 100 nm and the films deposited at laser-beam fluences below 0.7 J/cm² and annealed at 700°C had amorphous-like optical transmittance and low reflectance. A refractive index value $n \approx 2.1$ was calculated for the films annealed at 700°C, and the value was quite constant over the wavelength region from 450 to 750 nm. The extinction coefficient k decreased monotonically from 0.02 to 0.012 in this same wavelength range. The band-gap energy was around 3.5 eV.

4. Conclusions

Ferroelectric PNZT thin films were deposited using pulsed laser deposition. Afterwards, the films were post-annealed at different temperatures of 700, 800 and 900°C, respectively. The crystal structure, grain size distribution, surface morphology, and optical transmittance and reflectance spectra were measured from the films. PNZT

films annealed at 700°C, especially those which were deposited at laser-beam fluences below 0.7 J/cm², had a nano-crystalline structure with random grain orientation and quite poor surface morphology. On the other hand, the films annealed at higher temperatures, had a columnar microstructure where grains had an orientation with $\langle 001 \rangle$ direction perpendicular to the film surface. This structure started to grow from the upper surface of the film, and emerged through the film with increasing annealing temperature. Surface morphology of these films was also remarkably improved. Optical transmittance and the reflectance values also increased due to the improved microstructure of films and morphology of the film surfaces.

References

1. Meyer-Arendt, J. R., *Introduction to the Classical and Modern Optics*. Prentice-Hall, New Jersey, 1989 pp. 317–319.
2. Hideaki, A. and Kiyotaka, W., Sputtering preparation of ferroelectric PLZT thin films and their optical applications. *IEEE Trans. Ultrason. Ferroelectr. Freq. Control*, 1991, **38**, 645–655.
3. Peng, H. C., Chang, J.-F. and Desu, S. B., Optical properties of PZT, PLZT, and PNZT thin films. *Mater. Res. Soc. Symp. Proc.*, 1992, **243**, 21–26.
4. Dogheche, E., Jaber, B., Rémiens, D. and Thierry, B., Determination of optical properties of lead based ferroelectric thin films for integrated optics applications. *Microelectron. Eng.*, 1995, **29**, 315–318.
5. Majumder, S. B., Mohapatra, Y. N. and Agrawal, D. C., Optical and microstructural characterization of sol-gel derived cerium-doped PZT thin films. *J. Mater. Sci.*, 1997, **32**, 2141–2150.
6. Jaber, B., Dogheche, E., Rémiens, D. and Thierry, B., Influence of deposition parameters on physico-chemical and optical properties of sputtered PbTiO₃ thin films. *Integrated Ferroelectrics*, 1996, **13**, 225–237.
7. Lappalainen, J., Frantti, J. and Lantto, V., Effect of laser-ablation process parameters and post-annealing treatment on ferroelectric PZT thin films. *Applied Surface Science*, 1999, **142**, 407–412.
8. Lappalainen, J. and Lantto, V., Composition and phase structure in laser deposited and post-annealed $\text{Pb}_{1-3y/2}\text{Nd}_y(\text{Zr}_x\text{Ti}_{1-x})\text{O}_3$ thin films. *Applied Surface Science*, 2000, **154-155**, 118–122.
9. Lappalainen, J., Frantti, J. and Lantto, V., Surface structure and particulate generation in $\text{Pb}_{0.97}\text{Nd}_{0.02}(\text{Zr}_{0.55}\text{Ti}_{0.45})\text{O}_3$ ablation targets during pulsed laser deposition. *J. Am. Ceram. Soc.*, 1999, **82**, 889–896.
10. Lappalainen, J., Frantti, J. and Lantto, V., Electrical and mechanical properties of ferroelectric thin films laser ablated from $\text{Pb}_{0.97}\text{Nd}_{0.02}(\text{Zr}_{0.55}\text{Ti}_{0.45})\text{O}_3$ target. *J. Appl. Phys.*, 1997, **82**, 3469–3477.
11. Nilsson, P.-O., Determination of optical constants from intensity measurements at normal incidence. *Appl. Opt.*, 1968, **7**, 435–442.